1-11-2018

Physics of Hollow Bose-Einstein Condensates

Karmela Padavić
University of Illinois at Urbana-Champaign

Kuei Sun
University of Texas at Dallas

Courtney Lannert
Smith College, clannert@smith.edu

Smitha Vishveshwara
University of Illinois at Urbana-Champaign

Physics of hollow Bose-Einstein condensates

Karmela Padavić[1], Kuei Sun[2] [(a)], Courtney Lannert[3,4] [(b)] and Smitha Vishveshwara[1] [(c)]

[1] *Department of Physics, University of Illinois at Urbana-Champaign - Urbana, Illinois 61801-3080, USA*
[2] *Department of Physics, The University of Texas at Dallas - Richardson, Texas 75080-3021, USA*
[3] *Department of Physics, Smith College - Northampton, Massachusetts 01063, USA*
[4] *Department of Physics, University of Massachusetts - Amherst, Massachusetts 01003-9300, USA*

Abstract –Bose-Einstein condensate shells, while occurring in ultracold systems of coexisting phases and potentially within neutron stars, have yet to be realized in isolation on Earth due to the experimental challenge of overcoming gravitational sag. Motivated by the expected realization of hollow condensates by the space-based Cold Atomic Laboratory in microgravity conditions, we study a spherical condensate undergoing a topological change from a filled sphere to a hollow shell. We argue that the collective modes of the system show marked and robust signatures of this hollowing transition accompanied by the appearance of a new boundary. In particular, we demonstrate that the frequency spectrum of the breathing modes shows a pronounced depression as it evolves from the filled sphere limit to the hollowing transition. Furthermore, when the center of the system becomes hollow surface modes show a global restructuring of their spectrum due to the availability of a new, inner, surface for supporting density distortions. We pinpoint universal features of this topological transition as well as analyse the spectral evolution of collective modes in the experimentally relevant case of a bubble-trap.

Quantum matter, when subject to transitions of a topological nature, undergoes fundamental changes in its properties [1]. Such transitions involve singular deformations of the underlying space inhabited by the system, be it real or abstract. For instance, the ripping action required to convert a sphere into a torus. In topological materials, which have recently gained prominent attention, matter can transform from being a trivial insulator to one having gapless surface states. The topological nature of the transition can be pinpointed through the calculation or measurement of an abstract Berry phase type global invariant associated with non-trivial winding, for instance, in momentum space [2]. Cold atomic systems, given their spectacular trapping and tuning capabilities, not only enable measuring such topological invariants [3–5], they offer a much more direct, real space version of a topological transition through purely changing physical geometry. As a pioneering instance, the realization of toroidal Bose-Einstein condensates (BECs) [6,7] corresponds to a topological structure characterized by a homotopy group that is not equivalent to that of a disk. Here we explore salient features associated with the hollowing out of a spherically filled BEC and subsequent formation of a closed, hollow shell. The filled and hollow BECs are topologically inequivalent in that they correspond to different second homotopy groups. In other words, unlike for the filled spherically symmetric BEC, a spherical surface within the hollow BEC that surrounds its center cannot be continuously deformed into a point. In this sense, the hollowing of a condensate corresponds to a topological transition.

The study of hollow condensates is particularly germane now in light of the scheduled launch of the Cold Atomic Laboratory (CAL) [8] later this year aimed to investigate ultracold quantum gases aboard the International Space Station. One planned experiment on board involves the first creation of a hollow shell BEC [9,10] using an rf-dressed "bubble trap" potential [11]. While BECs have been produced in a host of interesting geometries [6,7,12–20], gravitational sag has prevented the realization of BEC shells on Earth [21,22]. Thus, microgravity environments, as expected to be produced in CAL and success-

[(a)]kuei.sun@utdallas.edu
[(b)]clannert@smith.edu
[(c)]smivish@illinois.edu

Karmela Padavić, Kuei Sun, Courtney Lannert, and Smitha Vishveshwara

fully demonstrated in the context of BECs in the ZARM drop tower in Germany [23] and in that of normal fluid shells during space shuttle launches [24], are necessary for the realization of hollow condensates. Shell-shaped BECs would be a test bed for quantum fluids in this topology, which naturally occurs in a number of diverse situations from laboratory-based micron scales to astronomical scales. In cold atomic systems, condensate shells are expected in Bose-Fermi mixtures [25–27] and optical-lattice "wedding-cake" structures [28–30] where Mott-insulating regions effectively trap superfluid layers [31]. In neutron stars, extremely high mass densities render ambient *relative* temperatures low enough for realizing macroscopic quantum states of matter, possibly giving rise to shells of differing states, some corresponding to superconductors and BECs of subatomic particles [32, 33].

Collective excitations offer an excellent probe of shape, boundary constraints, and topology, be they in solids, classical liquids, or quantum fluids. For instance, one "hears" the shape of a drum through its normal-mode oscillations [34, 35]. In trapped condensates, the low-lying excitations—their collective modes—were among the first phenomena to be studied after the initial realization of BECs [36–47]. Relevant to our studies, the topological change embodied in the emergence of an additional surface is significant for various physical systems. For example, for ships entering shallow water from the deep seas, the structure of water waves changes when the ocean floor emerges as a relevant boundary [48]. In the aforementioned space shuttle experiments [24] on normal fluid shells, sloshing modes show marked signatures of inner and outer boundaries, akin to those predicted in preliminary theoretical work on BEC shells [49]. Studies of two-dimensional annular BECs [50, 51] have revealed mode spectra that can distinguish an inner boundary in a non-destructive fashion. Such a collective mode analysis becomes even more pertinent for three-dimensional hollow condensates where direct imaging may not discern the presences of a hollow region. Here, we show that the collective mode spectrum presents a natural and powerful way to observe the topological change from filled to hollow in BECs, pinpointing universal features as well as making concrete predictions in experimentally relevant settings.

As we discuss in this Letter, the evolution of the collective mode frequencies as a function of a tuning parameter signals the appearance of a new boundary when a condensate undergoes the topological change of hollowing. The effect of the new inner boundary becomes manifest both in collective modes whose oscillations are primarily along the surface of the condensate (surface modes) as well as primarily transverse to it (breathing modes). In the former case of surface modes [Fig. 1(a)], such as high angular momentum modes in a sphere [52], density distortions exponentially decay into the bulk. When the new boundary appears, for any given surface mode, radial distortions are redistributed between the two boundaries. The frequency spectrum shows a sharp jump correspond-
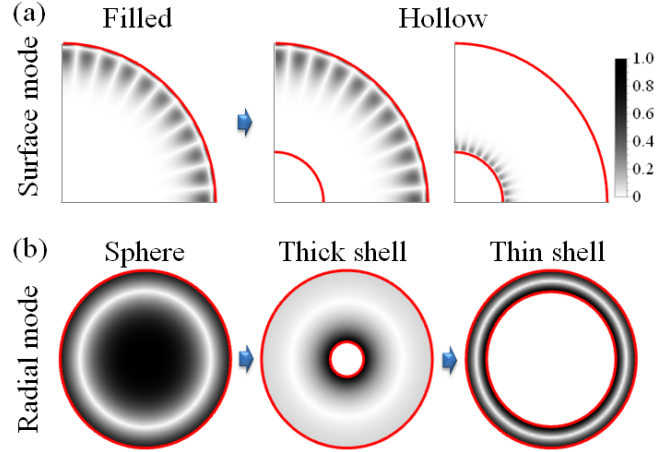

Fig. 1: (Color online) (a) Density variations of surface collective modes in the filled sphere (left), and hollow shell (middle and right), showing the bifurcation of modes confined to the inner and outer surfaces after the system hollows. (b) Density variation of breathing modes through the transition from filled sphere (left) to thin shell (right), showing the localization of mode amplitude to the (hollowing) center of the system during the transition. Surface (radial) modes profiles are presented in a quadrant (full) section of sphere and normalized as in the bar graph. The red solid curves indicate the (Thomas-Fermi) boundaries of the system.

ing to this redistribution—each boundary surface hosts fewer nodes of oscillation so the energy associated with a given oscillatory distortion is lowered.

For the latter case of transverse modes [Fig. 1(b)], of which the simplest is the spherically symmetric breathing mode [49, 53], the collective mode spectrum shows a distinct dip in frequency when the inner surface is created. Breathing modes localize near the new boundary as the condensate begins to hollow. Density and stiffness of the condensate in the center of the system as it hollows are very low, causing an unusually low oscillation frequency and an associated dip in the mode spectrum. We explicitly demonstrate these effects in the simplest case of spherical symmetry; our results are summarized in Figs. 2 and 4.

As is common and effective for collective mode analyses in BECs, we employ the hydrodynamic approach, which models excitations with relatively small, smooth deviations from the equilibrium density of the condensate. (Oscillations of certain low lying modes have been obtained by a variational approach in the literature [49] as well.) The collective eigenmode frequency ω is then related to density fluctuations in space and time via $\delta n(\mathbf{r}, t) = \delta n(\mathbf{r})e^{-i\omega t}$ [36, 54]. The eigenvalue equation for the collective modes and their frequencies is given by

$$-\frac{mS_l^2}{U}\omega^2\delta n = (\nabla n_{\mathrm{eq}}) \cdot (\nabla \delta n) + n_{\mathrm{eq}}\nabla^2\delta n, \qquad (1)$$

where the trapping potential enters through the equilibrium density profile, $n_{\mathrm{eq}}(\mathbf{r})$, m is the particle mass, S_l is the characteristic length for the trapping poten-

tial (in terms of which all lengths are measured below), and $U = 8\pi a_s/S_l$ is the interaction strength (proportional to the two-body scattering length a_s) [54]. In the presence of spherical symmetry the density fluctuation can be expanded in terms of spherical harmonics as $\delta n(\mathbf{r}) = D(r)Y_{\ell,m_\ell}(\theta,\phi)$ so that Eq. (1) reduces to

$$\frac{mS_l^2}{U}\omega^2 r^2 D = -\partial_r\left(r^2 n_{\mathrm{eq}}\partial_r D\right) + \ell(\ell+1)n_{\mathrm{eq}}D. \qquad (2)$$

The collective modes in a spherically symmetric system can be characterized by quantum numbers ν, ℓ, m_ℓ corresponding to the number of radial and angular nodes, respectively.

In our solution of the hydrodynamic equations below, we initially make the simplifying assumption that the condensate is strongly interacting in the sense that $Na_s/S_l \gg 1$ and that the associated Thomas-Fermi approximation holds. The Thomas-Fermi form for the equilibrium density depends on the trapping potential and the chemical potential, μ (determined by the net number of particles, N, in the condensate): $n_{\mathrm{eq}}(\mathbf{r}) = [\mu - V(\mathbf{r})]/U$. This approximation models a condensate having sharp boundaries identified by $V(\mathbf{r}) = \mu$, while in reality, the condensate density decreases gradually at its boundaries. We therefore use the Thomas-Fermi approximation to pinpoint signatures of hollowing, and extend our results to more physically realistic scenarios by treating the boundary of the condensate more accurately through numerics.

While we focus on universal collective mode features, in tandem, as a concrete example, we analyze the specific case of the spherical bubble trap, originally proposed by Zobay and Garraway [11]. This trapping potential allows for smooth tuning of the condensate shape between the filled sphere and hollow shell topology and has the form

$$V_{\mathrm{bubble}}(\mathbf{r}) = m\omega_0^2 S_l^2\sqrt{(r^2-\Delta)^2/4 + \Omega^2}. \qquad (3)$$

Here Δ and Ω are experimental parameters that can be precisely controlled. The minimum of this potential is found at $r_0 = \sqrt{\Delta}$. The filled sphere BEC geometry is realized when $\Delta = \Omega = 0$ since for this choice of parameters the bubble trap reduces to the harmonic trap: $V_0(\mathbf{r}) = \frac{1}{2}m\omega_0^2 S_l^2 r^2$. For large Δ (when r_0 is much larger than the thickness of the condensate shell), the bubble trap potential is approximated near its minimum by a radially-shifted harmonic trap $V_{\mathrm{sh}}(\mathbf{r}) = \frac{1}{2}m\omega_{\mathrm{sh}}^2 S_l^2(r-r_0)^2$ having frequency $\omega_{\mathrm{sh}} = \omega_0\sqrt{\Delta/\Omega}$. Below, we set $\Delta = \Omega$ for simplicity. Consequently, we see that increasing or decreasing the trap parameter Δ, at a constant chemical potential, results in a deformation between the filled and hollow condensate geometries.

Evolution of surface modes. – The effect of hollowing on surface modes of a spherical condensate can be gleaned from the eigenvalue equation for the collective mode frequencies, Eq. (2), in the limit of large angular momentum, $\ell \gg 1$. The centrifugal term $\ell(\ell+1)n_{\mathrm{eq}}$

dominates in this limit and is minimized at the condensate's outer surface (due to $n_{\mathrm{eq}} \sim 0$), and also the inner one in the hollow case, thus causing localization of large-ℓ density deviations to these surfaces. At the transition between a filled and a hollow condensate, the doubling of the surfaces available for excitations creates a redistribution of radial nodes—some of the nodes can localize in the vicinity of the new, inner surface. Consequently, since fewer nodes are compressed in each surface region, the frequency of any single mode (indexed by the total number of radial nodes ν) is reduced across the hollowing transition. To provide an intuitive physical picture, we note that a similar situation is found in the energy states of a quantum double-well potential as the minima are brought into alignment. At the point at which the minimum potential values are equal, the energy eigenvalue corresponding to ν nodes jumps to corresponding to two degenerate states having 2ν and $2\nu+1$ nodes (for instance, states having $\nu = 2$ and $\nu = 3$ radial nodes become nearly degenerate with the $\nu = 1$ state.) Here, the centrifugal term in Eq. (2) plays the role of the potential and, as we show below, the experimentally relevant bubble trap even supports the degeneracy exhibited by the simple double-well analogy.

More concretely, focusing on the two surfaces, the Thomas-Fermi approximation for the bubble trap identifies the inner and outer boundaries at the radii $r = R_{\mathrm{in}} = \sqrt{2\Delta - R^2}$ and $r = R_{\mathrm{out}} = R$, respectively. Linearizing the trapping potential at these boundaries gives the Thomas-Fermi equilibrium densities

$$n_{\mathrm{eq}}^{\mathrm{TF}}(x_{\mathrm{in,out}}) = -\frac{F_{\mathrm{in,out}}}{U}x_{\mathrm{in,out}}, \qquad (4)$$

with $F_{\mathrm{in,out}} = -\nabla V_{\mathrm{bubble}}(R_{\mathrm{in,out}})$ and $x_{\mathrm{in,out}}$ the local variable pointing along the direction of $F_{\mathrm{in,out}}$. This description of the condensate is appropriate when the trapping potential V_{bubble} varies slowly over a distance $\delta_{\mathrm{sm}} = [\hbar^2/(2m|F|)]^{1/3}$ from a condensate boundary. Consequently, such linearization is not appropriate in the very thin shell limit thus restricting Eq. (4) to hollow BECs of nontrivial thickness. In thin hollow condensates with thickness $\delta_{\mathrm{t}} < 2\delta_{\mathrm{sm}}$ surface modes confined to the inner and the outer boundary overlap and hence cannot be treated as strictly localized at either of these surfaces.

Surface mode frequencies for thick BEC shells can be derived from the master equation, Eq. (1), using these density profiles and the ansatz that the density distortions exponentially decay into the bulk [52].The resultant frequencies are given by $mS_l^2\omega_{\mathrm{in,out}}^2 = (1 + 2\nu_{\mathrm{in,out}})F_{\mathrm{in,out}}q_{\mathrm{in,out}}$ where $\nu_{\mathrm{in,out}}$ indicates the number of nodes of the collective mode confined to a particular condensate boundary in the direction transverse to its surface. The wavenumber associated with each surface mode is given by $q_{\mathrm{in,out}} = \ell/R_{\mathrm{in,out}}$. To be more precise, these surface mode frequencies read

$$\omega_{\mathrm{in,out}}^2 = \frac{\omega_0^2\ell(R^2-\Delta)}{\sqrt{(R^2-\Delta)^2/4 + \Omega^2}}(2\nu_{\mathrm{in,out}}+1). \qquad (5)$$

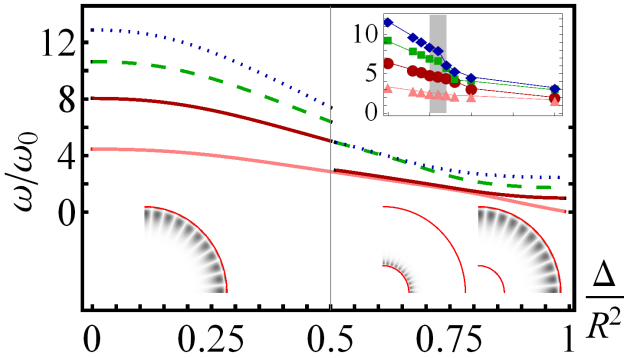Karmela Padavić, Kuei Sun, Courtney Lannert, and Smitha Vishveshwara

Fig. 2: (Color online) Oscillation frequencies of the $\ell = 20$ collective modes for the lowest four radial index values $\nu = 0, 1, 2, 3$ (curves from bottom to top, respectively) as the system is tuned from a filled sphere $\Delta = 0$ to a thin shell $\Delta \sim R^2$ at a constant chemical potential. The line through $\Delta = 0.5R^2$ (or the shaded region in the inset) demarcates the filled and hollow regions and the schematics along the bottom show the associated density deviations. Main: using the Thomas-Fermi approximation for the equilibrium density, which corresponds to sharp boundaries, and assuming the spatial extent of the condensate does not change, i.e., R is constant. Inset: using equilibrium profiles given by numerical solution of the GP equation (axes units are defined by the interaction energy $UN = 10^4$), which gives realistic soft boundaries, and assuming that the number of atoms making up the condensate, N, is constant.

We note that Eq. (5) is rather similar to the well-established result for the surface modes of a fully filled spherical condensate where $\omega_{sp}^2 = \ell \omega_0^2 (2\nu_{out} + 1)$ — the functional form and the ℓ dependence are the same up to numerical factors accounting for the finite thickness of the hollow shell BEC [52]. For the bubble trap, $F_{in} q_{in} = F_{out} q_{out}$ which leads to a degeneracy in the frequency of surface modes at the inner and outer surfaces, as noted above. A simple explanation for this degeneracy is that even though the inner surface is smaller in area, its lower stiffness can support more oscillations per unit distance (since $q_{in} > q_{out}$), bringing the frequency of oscillations with $\nu_{in} = \nu_{out}$ nodes on the two surfaces into alignment. We note that increasing the bubble trap parameter Δ decreases the thickness of the condensate shell and leads to coupling between the inner and outer boundary surface modes which can lift this degeneracy (as we will show in Fig. 2).

The restructuring of the surface mode spectrum following the hollowing out transition thus presents a marked contrast to the behavior of the same modes of a fully filled spherical BEC discussed in the literature [52]. We remark that inducing true surface modes corresponding to large ℓ values presents an experimental challenge, and is yet to be achieved even in the filled sphere case (although such modes have been experimentally observed in classical fluids [55]). But a comparison of the two cases highlights the difference between the collective mode spectra of filled and hollow BECs in any angular-momentum ℓ regime, includ-

ing the two extreme limits: $\ell = 0$ and $\ell \gg 1$. We proceed to discuss the $\ell = 0$ limit.

Evolution of breathing modes. – Collective modes involving density distortions transverse to the boundaries in a filled-sphere condensate correspond to spherically symmetric breathing modes. As the system evolves to a hollow shell, the density at the center of the system decreases, thus creating a region of low stiffness where density oscillations tend to localize and their frequency decreases. When the density in the center of the system vanishes, the inner boundary is created and the density deviations return to the bulk of the system. Thus, the hollowing transition and the appearance of an inner boundary are signaled by a prominent decrease in the transverse mode frequencies. More rigorously, in Eq. (1), the eigenfrequency receives two contributions: one proportional to the equilibrium density, n_{eq}, and the other to its gradient, ∇n_{eq}. In general, n_{eq} is smallest at the surface(s) of the BEC while ∇n_{eq} is smallest at the location of extremum density. The only situation in which both of these contributions can be small is at the hollowing-out transition: at the center of the system, where the inner boundary is emerging, both the condensate density and its gradient simultaneously vanish. The hydrodynamic equation therefore implies that the lowest frequency of oscillation for breathing modes can be realized close to the center of the condensate as it is starting to hollow. Consequently, the density deviations for the collective modes concentrate near the nascent inner surface and reach unprecedentedly low frequencies. The spectrum of the breathing modes, therefore, displays a minimum in frequency at the hollowing transition. Breathing modes exhibiting this non-monotonic spectral property are among the most experimentally accessible excitations of a three-dimensional spherically symmetric BEC and thus a good candidate for an observation of the effects of the hollowing-out transition. Additionally, collective modes with low angular momentum values, such as $\ell = 1$ or $\ell = 2$ exhibit similar frequency dip features. In fact, in a realistic experimental system that may lack perfect spherical symmetry, these low-ℓ collective modes would be the most likely candidate of study.

Numerical analyses for bubble-trap geometries. – Corroborating our heuristic arguments and simple derivations, we now perform an in-depth numerical analysis for collective modes in the bubble trap of Eq. (3) by directly solving the hydrodynamic equation of motion, Eq. (2) via a finite-difference method [56]. We initially use the Thomas-Fermi approximation for the equilibrium density (n_{eq}); this approach focuses on salient features of the topological hollowing transition by modeling a sharp inner (Thomas-Fermi) boundary. In these calculations we hold the outer radius of the condensate, R, fixed as Δ is changed. We then go beyond the Thomas-Fermi approximation by solving the time-independent Gross-Pitaevskii (GP) equation [54] for the equilibrium density, using an

imaginary-time algorithm [57]. Here, calculations are performed with a fixed number of atoms N in the condensate. This method addresses the fate of the mode spectra in the physically realistic case of soft condensate boundaries.

First addressing the surface modes, Fig. 2 shows the evolution of the collective mode spectrum obtained by direct numerical solution of Eq. (2) with $\ell = 20$, for a range of values of Δ in the bubble trap potential of Eq. (3), tuning from the fully filled sphere to thin shell limits. The transition point where an inner boundary first appears occurs at $R_{\rm in} = 0$ or $\Delta/R^2 = 0.5$. As argued on general grounds above, the transition from filled sphere to hollow shell is indeed signaled by a reduction in frequency for a given radial index and a sudden degeneracy between modes having radial indices 2ν and $2\nu+1$ (here, ν denotes the total number of radial zeros for a given collective mode). Density fluctuations on either side of the transition are schematically represented along the bottom of Fig. 2.

The results described above model a sudden change from the filled sphere to the shell topology through the appearance of the sharp inner boundary in the Thomas-Fermi approximation. In contrast, the inset to Fig. 2 shows the result of solving the hydrodynamic equation for the $\ell = 20$ collective modes using the numerically exact equilibrium density, $n_{\rm eq}$, obtained by solving the time-independent GP equation (with an interaction strength of $NU = 10^4$). This more realistic modeling of the gradually emerging inner surface yields a smearing of the sharp frequency discontinuity found in the Thomas-Fermi approximation as marked by the shaded region in the inset of the figure. Nevertheless, the frequency spectrum of the collective modes still displays a notable jump and near-degeneracy of modes as the inner boundary emerges.

To corroborate our description of the frequency restructuring across the hollowing transition, in Fig. 3 we present the density deviations and radial node redistribution in the illustrative example of surface modes having $\ell = 20$ and $\nu = 1, 2$ and 3 on either side of the topological transition. Comparing Figs. 3 (a), (c) and (d), it is clear that after the emergence of the condensate's inner boundary, both modes with total number of radial nodes $\nu = 2$ and $\nu = 3$ bear similarity, in density deviations, to the mode with $\nu = 1$ radial nodes before this boundary surface was available. Additional nodes for $\nu = 2$ and $\nu = 3$ collective modes are present but appear as radial oscillations of small amplitude on a boundary surface opposite to the one with the most prominent nodal structure. After the hollowing change, the overall oscillation frequencies of the $\nu = 2$ and $\nu = 3$ collective modes are accordingly dominated by a single node associated with high amplitude radial motion. As this motion has the highest energetic cost, these frequencies are nearly equivalent to the oscillation frequency of the collective mode with a single radial node in the fully filled spherical condensate. We emphasize that this is a feature that only occurs once the system is hollow, as demonstrated by a comparison of Figs. 3 (a) and (b)—collective modes with $\nu = 1$ and $\nu = 2$ radial nodes
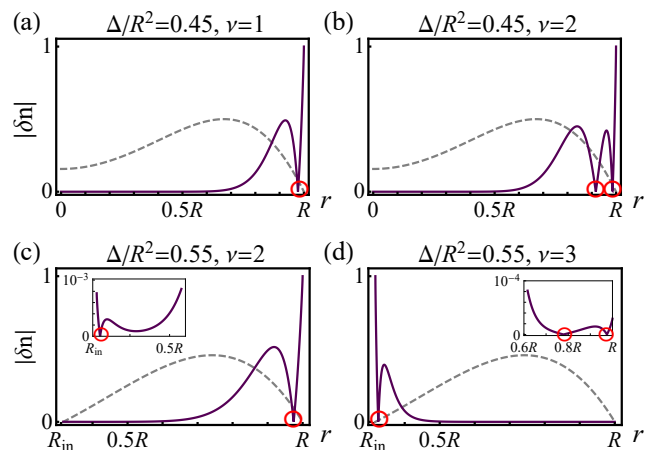

Fig. 3: (Color online) Normalized density deviation profiles $|\delta n(r)|$ along the radial direction of surface collective modes ($\ell = 20$) in filled (a,b) and hollow (c,d) condensates with $\Delta/R^2 = 0.45$ and 0.55, respectively, for varying number of radial nodes ν, as denoted. The density deviation profile and radial node (circled) structure of $\nu = 1$ in the filled case resembles that of $\nu = 2$ and $\nu = 3$ in the hollow case close to the outer and inner boundaries, respectively. In the barely hollow situation shown, the centrifugal barrier given by $\ell(\ell + 1)n_{\rm eq}$ in Eq. (2) – and represented by the dotted line (in arbitrary units) – is lowered so as to distribute the remaining nodes of the $\nu = 2$ and $\nu = 3$ to the other surface as small oscillations [insets in (c,d)].

have rather different radial profiles for a fully filled spherical BEC. Extrapolating to more general surface modes, this redistribution of nodes explains the jump in the frequency spectrum shown in Fig. 2 where collective modes with total 2ν and $2\nu + 1$ radial nodes after the hollowing transition smoothly continue the spectrum of the ν surface mode of the BEC prior to hollowing.

In Fig. 4, to exhibit the behavior of the breathing modes, we show the results of the direct numerical solution of Eq. (2) for the case $\ell = 0$ as the parameter Δ is varied. We note the sharp depression of the frequencies at the transition point and their otherwise smooth evolution to the solid-sphere and thin-shell limits at $\Delta/R^2 = 0$ and 1, respectively. Additionally, we note that the density deviation for these spherically symmetric modes, as shown along the bottom of Fig. 4, displays confinement to the inner boundary at the transition from filled to hollow. As with the surface modes, we expect this sudden transition to be replaced by a smoother crossover in a realistic system in which the condensate's boundaries are not sharp. In the inset to Fig. 4, we show the result of solving the hydrodynamic equation for the $\ell = 0$ collective modes using the numerical solution to the time-independent GP equation for the equilibrium density, $n_{\rm eq}$. While in this more realistic situation the transition is gradual, as indicated by the shaded region in the inset of Fig. 3, the characteristic decrease in frequency from the filled sphere through the transition point clearly persists, indicating that the
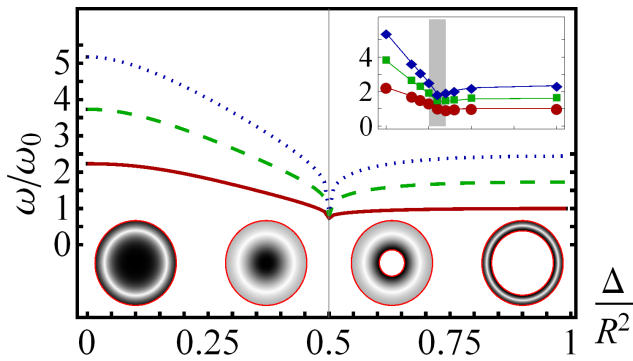
Fig. 4: (Color online) Oscillation frequencies of the lowest three breathing ($\ell = 0$) collective modes $\nu = 1, 2, 3$ (curves from bottom to top) as Δ is varied from the filled-sphere to the thin-shell limit at a constant chemical potential, in the Thomas-Fermi approximation with constant R (main) and using the numerically exact equilibrium densities with constant N (inset). The line through $\Delta = 0.5R^2$ (or the shaded region in the inset) demarcates the filled and hollow regions and the schematics along the bottom show the associated density deviations, for (from left to right) $\Delta/R^2 = 0$, 0.45, 0.55, and 0.8.

hollowing at the center of the condensate can be observed through the spectrum of the system's breathing modes. Additionally, since the decrease in central density here occurs less sharply than when the Thomas-Fermi approximation is used, the frequency curves in the inset of Fig. 4 decrease to distinct values at the hollowing transition, in contrast to their near-degeneracy in the Thomas-Fermi approximation.

To summarize, we have explored the physics of a BEC undergoing a topological change from a filled sphere to a hollow shell and shown that the collective modes are powerful indicators of such a transition. In particular, spherically symmetric breathing modes show a crossover between the fully filled and thin shell limits at the hollowing-out point where the associated frequency spectrum exhibits a tell-tale dip. High-angular-momentum surface modes show marked sensitivity to the appearance of a new boundary as well.

We now turn to the analogous lower-dimensional BEC geometry of a disk hollowing out into an annulus, effectively represented by a toroidal geometry. Both structures have been well-studied theoretically [50, 51] and experimentally [6, 7]. The transition regime between the two topologies has yet to be studied and is potentially experimentally more tracatable than the three-dimensional spherical case. We have performed preliminary collective mode spectral analyses for the disk-annulus system using the same techniques as those presented here. Our main results for the spherical case hold equally well for the two dimensional system, given the common physics (vanishing of central density at the hollowing out transition and so on). Specifically, the breathing modes show a

dip and surface modes a reconfiguration of radial nodes in their frequency spectra around the topological transition from a disk to an annulus. While the shell and the annulus topologies host similar collective modes when their thickness is small [50], the collective mode frequencies in the overall hollow regimes differ. Moreover, the collective mode spectra cannot distinguish the different topological measures of the BEC's shape such as the fundamental group for the disk-annulus transition (determined by whether or not a loop can be shrunk to a point) or the second homotopy group for the sphere-shell transition (determined by whether a spherical surface can be shrunk to a point). However, we note that a fundamental difference exists between the two cases, making the study of collective mode spectra more pressing in the three-dimensional case: in two dimensions, the presence of a hollow inner region can be imaged (and visualized) directly by absorption imaging techniques. However, for the spherical geometry, direct imaging of the hollow region is obstructed by the presence of a surrounding condensate in all three dimensions, rendering collective mode spectra a powerful, non-destructive probe of the hollowing transition.

Finally, the CAL trap experiment is expected to pioneer the realization of condensate shells thus adding to the growing interest in BECs in microgravity conditions in space [58] and Earth-based environments [23]. The challenge has been that under typical terrestrial experimental conditions, gravitational sag causes heavy depletion at the shell's apex and a pooling of atoms at its bottom. Excluding gravitational effects, we estimate that for a BEC of $\sim 10^5$ ^{87}Rb atoms forming a cloud of 10 μm in a harmonic trap of bare frequency 500 Hz, in the transition from the filled sphere to the thin shell limit the lowest breathing (surface) mode would evolve from about 1 (4) kHz to 0.5 kHz, which are in an accessible regime and in a large enough range to probe our predictions. We predict the decrease in the collective mode frequency at the hollowing point, compared to the oscillation frequency of the same mode in the fully filled spherical BEC to be rather prominent, on the order of 50% or more, for all low-lying breathing (and low-ℓ) modes. Somewhat higher modes, such as $\nu = 3$, are suitable for for experimental detection of the diminishing of collective mode frequency at the hollowing point compared to the thin-shell limit as well. For instance, the collective mode with $\nu = 3$ shows a 20% change between these two regimes, which makes it a good candidate for a full observation of the non-monotonicity of the collective mode frequency spectrum at the hollowing point. Further work on BEC shells from collective mode behavior, expansion and time-of-flight, and the nature of vortices in this new geometry is in order. These studies are relevant to situations ranging from the microscopic scale of the CAL trap experiments to the proposed existence of BEC shells in stellar objects and would deepen our insight into topological changes in quantum systems.

∗ ∗ ∗

REFERENCES

[1] J. M. Kosterlitz and D. J. Thouless, Ordering, metastability and phase transitions in two-dimensional systems, J. Phys. C: Solid State Phys. **6**, 1181 (1973); F. D. M. Haldane, Nonlinear Field Theory of Large-Spin Heisenberg Antiferromagnets: Semiclassically Quantized Solitons of the One-Dimensional Easy-Axis Néel State, Phys. Rev. Lett. **50**, 1153 (1983).

[2] M. Z. Hasan and C. L. Kane, Topological Insulators, Rev. Mod. Phys. **82**, 3045 (2010); X.-L. Qi and S.-C. Zhang, Topological Insulators and Superconductors, Rev. Mod. Phys. **83**, 1057 (2011); C.-K. Chiu, J. C. Y. Teo, A. P. Schnyder, and S. Ryu, Classification of topological quantum matter with symmetries, Rev. Mod. Phys. **88**, 035005 (2016).

[3] M. Atala, M. Aidelsbrger, J. T. Barreiro, D. Abanin, T. Kitagawa, E. Demler and I. Bloch, Direct measurements of the Zak phase in topological Bloch bands, Nat. Phys. **9**, 795 (2013).

[4] P. Delplace, D. Ullmo and G.Montambaux, Zak phase and the existence of edge state in graphene, Phys. Rev. B **84**, 195452 (2011).

[5] H. M. Price and N. R. Cooper, Effects of Berry Curvature on the Collective Modes of Ultracold Gases Phys. Rev. Lett. **111**, 220407 (2013).

[6] S. Gupta, K. W. Murch, K. L. Moore, T. P. Purdy, and D. M. Stamper-Kurn, Bose-Einstein Condensation in a Circular Waveguide, Phys. Rev. Lett. **95**, 143201 (2005).

[7] A. Ramanathan, K. C. Wright, S. R. Muniz, M. Zelan, W. T. Hill, III, C. J. Lobb, K. Helmerson, W. D. Phillips, and G. K. Campbell, Superflow in a Toroidal Bose-Einstein Condensate: An Atom Circuit with a Tunable Weak Link, Phys. Rev. Lett. **106**, 130401 (2011).

[8] http://coldatomlab.jpl.nasa.gov

[9] N. Lundblad, private communication (2015).

[10] N. Lundblad, T. Jarvis, D. Paseltiner, and C. Lannert, Progress toward studies of bubble-geometry Bose-Einstein condensates in microgravity with a ground-based prototype of NASA CAL, DAMOP Meeting, K1.00119 (2016).

[11] O. Zobay and B. M. Garraway, Two-Dimensional Atom Trapping in Field-Induced Adiabatic Potentials, Phys. Rev. Lett. **86**, 1195 (2001); Atom trapping and two-dimensional Bose-Einstein condensates in field-induced adiabatic potentials, Phys. Rev. A **69**, 023605 (2004).

[12] A. Gorlitz, J.M. Vogels, A. E Leanhardt, C. Raman, T. L. Gustavson, J. R. Abo-Shaeer, A. P. Chikkatur, S. Gupta, S. Inouye, T. Rosenband, and W. Ketterle, Realization of Bose-Einstein Condensates in Lower Dimensions, Phys. Rev. Lett. **87**, 130402 (2001).

[13] M. Greiner, I. Bloch, O. Mandel, T. W. Hansch, and T. Esslinger, Exploring Phase Coherence in a 2D Lattice of Bose-Einstein Condensates, Phys. Rev. Lett. **87**, 160405 (2001).

[14] S. Dettemer, D. Hellweg, P. Ryytty, J. J. Arlt, W. Ermer, K. Sengstock, D. S. Petrov, G. V. Shlyapnikov, H. Kreutzmann, L. Santos, and M. Lewenstein, Observation of Phase Fluctuations in Elongated Bose-Einstein Condensates, Phys. Rev. Lett. **87**, 160406 (2001).

[15] G. Hechenblaikner, J. M. Krueger, and C. J. Foot, Properties of quasi-two-dimensional Condensates in Highly Anisotropic Traps, Phys. Rev. A **71**, 013604 (2005).

[16] N. L. Smith, W. H. Heathcote, G. Hechenblaikner, E. Nugent, and C. J. Foot, Quasi-2D Confinement of a BEC in a Combined Optical and Magnetic Potential, J. Phys. B **38**, 223 (2005).

[17] A. L. Gaunt, T. F. Schmidutz, I. Gotlibovych, R. P. Smith, and Z. Hadzibabic, Bose-Einstein Condensation of Atoms in a Uniform Potential, Phys. Rev. Lett. **110**, 200406 (2013).

[18] A. Smerzi, S. Fantoni, S. Giovanazzi, and S. R. Shenoy, Quantum Coherent Atomic Tunneling between Two Trapped Bose-Einstein Condensates, Phys. Rev. Lett. **79**, 4950 (1997).

[19] Y. Shin, M. Saba, T. A. Pasquini, W. Ketterle, D. E. Pritchard, and A. E. Leanhardt, Atom Interferometry with Bose-Einstein Condensates in a Double-Well Potential, Phys. Rev. Lett. **92**, 050405 (2004).

[20] S. Hofferberth, I. Lesanovsky, B. Fischer, J. Verdu, and J. Schmiedmayer, Radiofrequency-dressed-state Potentials for Neutral Atoms, Nat. Phys. **2**, 710 (2006).

[21] Y. Colombe, E. Knyazchyan, O. Morizot, B. Mercier, V. Lorent, and H. Perrin, Ultracold atoms confined in rf-induced two-dimensional trapping potentials, EPL **67**, 593 (2004).

[22] K. Merloti, R. Dubessy, L. Longchampon, A. Perrin, P.-E. Pottie, V. Lorent, and H. Perrin, A two-dimensional quantum gas in a magnetic trap, New J. Phys. **15**, 033007 (2013).

[23] http://www.zarm.uni-bremen.de/drop-tower.html

[24] T. G. Wang, A. V. Anilkumar, C. P. Lee and K. C. Lin, Core-centering of Compound Drops in Capillary Oscillations: Observations on USML-1 Experimets in Space, J. Colloid Interface Sci **165**, 1 (1994).

[25] K. Mølmer, Bose Condensates and Fermi Gases at Zero Temperature, Phys. Rev. Lett. **80**, 1804 (1998).

[26] S. Ospelkaus, C. Ospelkaus, L. Humbert, K. Sengstock, and K. Bongs, Tuning of Heteronuclear Interactions in a Degenerate Fermi-Bose Mixture, Phys. Rev. Lett. **97**, 120403 (2006).

[27] B. V. Schaeybroeck and A. Lazarides, Trapped phase-segregated Bose-Fermi mixtures and their collective excitations, Phys. Rev. A **79**, 033618 (2009).

[28] G. Batrouni, V. Rousseau, R. Scalettar, M. Rigol, A. Muramatsu, P. Denteneer, and M. Troyer, Mott Domains of Bosons Confined on Optical Lattices, Phys. Rev. Lett. **89** 117203 (2002).

[29] B. DeMarco, C. Lannert, S. Vishveshwara, and T.-C. Wei, Structure and stability of Mott-insulator shells of bosons trapped in an optical lattice, Phys. Rev. A **71**, 063601

(2005).

[30] G. K. Campbell, J. Mun, M. Boyd, P. Medley, A. E. Lean-hardt, L. G. Marcassa, D. E. Pritchard, and W. Ketterle, Imaging the Mott Insulator Shells by Using Atomic Clock Shifts, Science **313**, 649 (2006).

[31] R. A. Barankov, C. Lannert, and S. Vishveshwara, Co-existence of superfluid and Mott phases of lattice bosons, Phys. Rev. A **75**, 063622 (2007); K. Sun, C. Lannert, and S. Vishveshwara, Probing condensate order in deep optical lattices, Phys. Rev. A **79**, 043422 (2009).

[32] F. Weber, Strange quark matter and compact stars, Prog. Part. Nucl. Phys. **54**, 193 (2004).

[33] C. J. Pethick, T. Schaefer, and A. Schwenk, Bose-Einstein condensates in neutron stars, arXiv:1507.05839.

[34] M. Kac, Can One Hear the Shape of a Drum?, Am. Math. Monthly **73**, 1 (1966).

[35] O. Giraud and K. Thas, Hearing shapes of drums: Math-ematical and physical aspects of isospectrality, Rev. Mod. Phys. **82**, 2213 (2010).

[36] S. Stringari, Collective Excitations of a Trapped Bose-Condensed Gas, Phys. Rev. Lett. **77**, 2360 (1996).

[37] D. S. Jin, J. R. Ensher, M. R. Matthews, C. E. Wie-man, and E. A. Cornell, Collective Excitations of a Bose-Einstein Condensate in a Dilute Gas, Phys. Rev. Lett. **77**, 420 (1996).

[38] M.-O. Mewes, M. R. Andrews, N. J. van Druten, D. M. Kurn, D. S. Durfee, C. G. Townsend, and W. Ketterle, Collective Excitations of a Bose-Einstein Condensate in a Magnetic Trap, Phys. Rev. Lett. **77**, 988 (1996).

[39] M. Edwards, P. A. Ruprecht, K. Burnett, R. J. Dodd, and C. W. Clark, Collective Excitations of Atomic Bose-Einstein Condensates, Phys. Rev. Lett. **77**, 1671 (1996).

[40] Y. Castin and R. Dum, Bose-Einstein Condensates in Time Dependent Traps, Phys. Rev. Lett. **77**, 5315 (1996).

[41] D. M. Stamper-Kurn, H.-J. Miesner, S. Inouye, M. R. Andrews, and W. Ketterle, Collisionless and Hydrody-namic Excitations of a Bose-Einstein Condensate, Phys. Rev. Lett. **81**, 500 (1998).

[42] F. Chevy, V. Bretin, P. Rosenbusch, K. W. Madison, and J. Dalibard, Transverse Breathing Mode of an Elongated Bose-Einstein Condensate, Phys. Rev. Lett. **88**, 250402 (2002).

[43] C. Fort, F. S. Cataliotti, L. Fallani, F. Ferlaino, P. Maddaloni, and M. Inguscio, Collective Excitations of a Trapped Bose-Einstein Condensate in the Presence of a 1D Optical Lattice, Phys. Rev. Lett. **90**, 140405 (2003).

[44] L. Yang, X.-R. Wang, Ke Li, X.-Z. Tan, H.-W. Xiong, and B.-L. Lu, Low-Energy Collective Excitation of Bose-Einstein Condensates in an Anisotropic Magnetic Trap, Chin. Phys. Lett. **26**, 076701 (2009).

[45] E. Haller, M. Gustavsson, M. J. Mark, J. G. Danzl, R. Hart, G. Pupillo, and H.-C. Nägerl, Realization of an Ex-cited, Strongly Correlated Quantum Gas Phase, Science **325**, 1224 (2009).

[46] S. E. Pollack, D. Dries, R. G. Hulet, K. M. F. Magalhães, E. A. L. Henn, E. R. F. Ramos, M. A. Caracanhas, and V. S. Bagnato, Collective excitation of a Bose-Einstein con-densate by modulation of the atomic scattering length, Phys. Rev. A **81**, 053627 (2010).

[47] T. Kuwamoto and T. Hirano, Collective Excitation of Bose-Einstein Condensates Induced by Evaporative Cool-ing, J. Phys. Soc. Jpn. **81**, 074002 (2012).

[48] J. Lighthill Waves in Fluids, (Cambridge University Press, Cambridge, 1978).

[49] C. Lannert, T.-C. Wei and S. Vishvehswara, Dynamics of condensate shells: Collective modes and expansion, Phys. Rev. A **75**, 013611, (2007).

[50] M. Cozzini, B. Jackson, and S. Stringari, Vortex Signa-tures in Annular Bose-Einstein Condensates, Phys. Rev. A **73**, 013603 (2006).

[51] R. Dubessy, T. Liennard, P. Pedri, and H. Perrin, Critical Rotation of an Annular Superfluid Bose-Einstein Conden-sate, Phys. Rev. A **86**, 011602(R) (2012).

[52] U. Al Khawaja, C. J. Pethick, and H. Smith, Surface of a Bose-Einstein condensed atomic cloud, Phys. Rev. A **60**, 1507 (1999).

[53] D. S. Lobser, A. E. S. Barentine, E. A. Cornell, and H. J. Lewandowski, Observation of a persistent non-equilibrium state in cold atoms, Nat. Phys. **11**, 1009 (2015); C. J. E. Straatsma, V. E. Colussi, M. J. Davis, D. S. Lobser, M. J. Holland, D. Z. Anderson, H. J. Lewandowski, and E. A. Cornell, Collapse and revival of the monopole mode of a degenerate Bose gas in an isotropic harmonic trap, Phys. Rev. A **94**, 043640 (2016).

[54] C. J. Pethick and H. Smith, Bose-Einstein Condensa-tion in Dilute Gases, 2st, ed. (Cambridge University Press, Cambridge, 2008).

[55] P. Brunet and J. H. Snoeijer, Star-drops formed by peri-odic excitation and on an air cushion – A shot review, EPJ ST **192**, 1 (2011)

[56] G. D. Smith, Numerical solution of partial differential equations: finite difference methods (Oxford university press, 1985).

[57] M. L. Chiofalo, S. Succi, and M. P. Tosi, Ground state of trapped interacting Bose-Einstein condensates by an ex-plicit imaginary-time algorithm, Phys. Rev. E **62**, 7438 (2000).

[58] https://www.zarm.uni-bremen.de/en.html